

On the difference between Herbig Ae and Herbig Be stars

J.C. Mottram^{1*}, J.S. Vink^{2,3}, R.D. Oudmaijer¹, M. Patel^{1,3}

¹*Department of Physics and Astronomy, University of Leeds, Leeds LS2 9JT, UK*

²*Lennard-Jones Laboratory, Astrophysics, Keele University, Keele ST5 5BG, UK*

³*Imperial College London, Blackett Laboratory, Prince Consort Road, London SW7 2AZ*

Accepted 2007 March 3. Received 2007 January 5; in original form 2006 October 4

ABSTRACT

We present linear spectropolarimetric data for eight Herbig Be and four Herbig Ae stars at $H\alpha$, $H\beta$ and $H\gamma$. Changes in the linear polarisation are detected across all Balmer lines for a large fraction of the observed objects, confirming that the small-scale regions surrounding these objects are flattened (i.e. disk-like). Furthermore, all objects with detections show similar characteristics at the three spectral lines, despite differences in transition probability and optical depth going from $H\alpha$ to $H\gamma$. A large fraction of early Herbig Be stars (B0-B3) observed show line depolarisation effects. However the early Herbig Ae stars (A0-A2), observed for comparison, show intrinsic line polarisation signatures. Our data suggest that the popular magnetic accretion scenario for T Tauri objects may be extended to Herbig Ae stars, but that it may not be extended to early Herbig Be stars, for which the available data are consistent with disc accretion.

Key words: Techniques: spectropolarimetry - circumstellar matter - Stars: emission-line, Herbig, Be - Stars: formation - Stars: pre-main-sequence

1 INTRODUCTION

While magnetic T-Tauri type models for low-mass star formation have been reasonably well accepted, there is currently no such picture for the early evolutionary phases of higher mass stars. Many questions, such as whether higher mass stars form via disc accretion, and issues relating to the importance of magnetic fields during high-mass star formation, remain open. Herbig Ae/Be stars are of considerable interest in attempts to resolve these questions, as they are young stars of intermediate mass (2 - 15 M_{\odot}) at the interface between low and high-mass star formation. In addition, Herbig Ae/Be stars are the most massive stars with a visible pre-main sequence phase.

T Tauri stars have relatively strong magnetic fields (Johns-Krull et al. 1999; Symington et al. 2005) and these fields have important physical effects on the accretion flow. It is generally believed that magnetic fields play a lesser role for stars more massive than the Sun, as stars at spectral types A and earlier lack convective outer mantles.

The picture of the role of magnetic accretion as a function of spectral type changed when Vink et al. (2002) found that a large fraction (9/11) of Herbig Ae stars show changes in the linear polarisation intrinsic to the $H\alpha$ line (extended to 10/13 with data from Vink et al. 2005a) – similar to the

fraction (9/10) of such intrinsic line effects in T Tauri stars (Vink et al. 2005a). The origin for these $H\alpha$ line effects in both T Tauri and Herbig Ae stars is believed to be the result of the fact that *emission line* photons from the central object are scattered off a rotating accretion disc with an inner hole (Vink et al. 2005b). From here the material is probably funnelled along magnetic field lines (Wade et al. 2005; Hubrig et al. 2006), onto the stellar surface.

Early Herbig Be stars (spectral types B0-B5, see Natta et al. 2001) show very different behaviour in their $H\alpha$ polarimetry. Although the frequency of observed effects is high (7/12; Vink et al. 2002), and wholly consistent with all Herbig Be stars being embedded in flattened circumstellar media (c.f. classical Be stars), their $H\alpha$ polarisation behaviour is very different from that of Herbig Ae/T Tauri stars, as it is not the line but the continuum that is found to be polarised, with the $H\alpha$ line “depolarised” with respect to the continuum (Oudmaijer & Drew 1999). So, in summary, the emission line photons are intrinsically polarised compared to the continuum for Herbig Ae and T Tauri stars, but are depolarised relative to the continuum for Herbig Be stars.

The difference in the behaviour of the linear polarisation across $H\alpha$ between the Herbig Be and Ae stars may be an indication that there is a transition in the Hertzsprung-Russell Diagram from magnetic accretion at spectral type A to disc accretion at spectral type B. However, alternatively,

* E-mail:jcm@ast.leeds.ac.uk

Table 1. Herbig Ae/Be observations. Columns 2 & 3 show the logarithmic average of the two photometric magnitude measurements in the relevant band by Monet et al. (2003). Spectral types (column 4) are taken from references in Thé et al. (1994). The exposure time (columns 7 & 8) consists of an integer multiple of 4 spectra (one for each half-wave plate position) multiplied by the exposure time of an individual spectrum.

Object Name	Mag.		Sp. Type	Date		Exposure(s)		
	<i>R</i>	<i>B</i>		<i>R</i>	<i>B</i>	<i>R</i>	<i>B</i>	
MWC 166	6.90	7.35	B0 IV	30/12/96 + 01/01/97*		29/09/04	—	480
MWC 1080	11.02	13.28	B0	—	29/09/04	28/09/04	—	4320
GU CMa	6.64	6.67	B2 V	11/07/95*	29/09/04	28/09/04	—	720
MWC 361	7.27	7.69	B2V	18/12/99*	29/09/04	28/09/04	—	1600
II Cep	9.03	9.80	B2 IV–V	19/12/99*	29/09/04	29/09/04	—	1440
BD +404124	10.53	11.37	B2	19/12/99*	29/09/04	28/09/04	—	2160
ω Ori	4.56	4.38	B3 III–IV	11/01/95*	29/09/04	28/09/04	—	144
MWC 147	8.73	9.06	B6 V	18/12/99*	29/09/04	28/09/04	—	1920
AB Aur	7.03	7.15	A0 V	18/12/99*	30/09/04	30/09/04	—	1920
MWC 120	7.92	7.95	A0	29/09/04	30/09/04	29/09/04	1080	2640
MWC 480	7.63	7.91	A2	30/09/04	30/09/04	30/09/04	1800	1320
XY Per	9.41	10.04	A2 II	20/12/99*	29/09/04	29/09/04	—	1200

* Data from Vink et al. (2002), • data from Oudmaijer & Drew (1999)

Vink et al. (2002) considered the option that the compact polarised $H\alpha$ emission occurring in the Herbig Ae and T Tauri stars may be masked in the Herbig Be stars due to their much higher levels of $H\alpha$ emission.

We therefore designed an observational test to distinguish between these two options. The test involves linear spectropolarimetry across less opaque, higher excitation emission lines that can be expected to arise in the same location as the compact $H\alpha$ component that causes the line polarisation in the Herbig Ae stars. If the extension and optical depth of $H\alpha$ emission masks the evidence for a compact source in Herbig Be stars, then higher Balmer ($H\beta$ and $H\gamma$) observations should reveal position angle rotations (QU loops) in the Herbig Be group. However, if these angle rotations are not observed at these lines in the Herbig Be population, while they do appear at $H\alpha$ among the Herbig Ae stars, this would suggest that the circumstellar environments of Herbig Be stars are physically different from those of Herbig Ae stars.

The goal of this paper is thus to perform spectropolarimetry of $H\beta$ and $H\gamma$ observations in early Herbig Be stars. The paper proceeds as follows: we begin by discussing the observations and data reduction in §2, then we discuss the results in §3 before providing discussion of these results and concluding remarks in §4. Detailed comments of the results for each object in our sample are presented in Appendix A, divided between Herbig Be stars (§ A1) and Herbig Ae stars (§ A2) in our sample.

2 OBSERVATIONS & DATA REDUCTION

The linear spectropolarimetric data were taken using the 4.2m William Herschel Telescope (WHT), La Palma over 3 nights in late September 2004. The ISIS spectrograph, a calcite block, and a rotating half-wave plate were used for the observations, as well as a dekker and slit. The dekker had three 5" holes, separated by 18", while a 1" slit width

was used for all object observations. The calcite block acted to separate the incoming light into two perpendicular rays, the O (ordinary) and E (extraordinary) rays, so one image contains a set of O and E rays for the image and two sets for the sky. Rotation of the half-wave plate then allowed measurement of the polarisation at the angles 0° , 45° , 22.5° and 67.5° . One complete data set is therefore formed by combining four images, one at each of the four angles mentioned above.

All bright early Herbig Be stars (from the catalogue by Thé et al. 1994) visible from La Palma in September 2004 were observed. We note that we strictly stick to their criteria, even though the evolutionary status of objects like ω Ori is debated. These data were supplemented by four Herbig Ae stars with similar criteria, as a basis for comparison.

The data includes images in both the *B* (4295–4955 Å) and *R* (6150–6815 Å) bands, with mean wavelength dispersions of 0.22 Å/pixel and 0.45 Å/pixel respectively. For the *B* band data, the R1200B grating and the 4096x2048 pixel EEV12 CCD detector on the ISIS Blue Arm were used, resulting in a spectral resolution (measured from arc lines) of 51 km/s around $H\beta$. In the *R* band, observations were taken using the R1200R grating and the MARCONI2 CCD on the ISIS Red Arm, resulting in a spectral resolution of 34 km/s around $H\alpha$. In order to eliminate instrumental asymmetry, observations for each object were taken with the object in the A (left most) and B (central) dekker holes. The dekker hole C was not used for object observations, but the sky was always measured at either A or B, whichever was not being used for the target. Care was taken not to saturate the CCD for objects with particularly strong emission lines by taking short exposures. The seeing on the first two nights was fair ($< 1.7''$) but became poor ($> 2''$) on the third night due to clouds.

Data reduction was carried out on each image frame using the Figaro software maintained by Starlink, and consisted of bias subtraction, cosmic ray removal, bad pixel correction, spectrum straightening and flat fielding. Wavelength

Table 2. Continuum polarisation measurements. Column 2 is the same as column 4 in Table 1. The continuum polarisation (columns 3 & 4) and polarisation angle (columns 5 & 6) were measured over the ranges (6150–6540 Å, 6580–6815 Å) and (4295–4310 Å, 4370–4840 Å, 4890–4955 Å) for R and B respectively. Systematic errors in %P and Θ are estimated at ~ 0.1 per cent.

Object Name	Sp. Type	$P_{cont}(\%)$		$\Theta_{cont}(\circ)$	
		R	B	R	B
MWC 166	B0 IV	$0.49 \pm 0.01^\bullet$	0.37 ± 0.01	$44.9 \pm 0.1^\bullet$	37.2 ± 0.5
MWC 1080	B0	–	1.71 ± 0.02	–	72.2 ± 0.3
		1.51 ± 0.01	1.99 ± 0.02	77.2 ± 0.1	72.1 ± 0.3
GU CMa	B2 V	$1.15 \pm 0.01^\bullet$	1.25 ± 0.01	$18.9 \pm 0.1^\bullet$	17.2 ± 0.1
MWC 361	B2V	$0.82 \pm 0.01^*$	0.88 ± 0.01	$95.6 \pm 0.1^*$	96.4 ± 0.1
II Cep	B2 IV–V	$4.24 \pm 0.01^*$	4.18 ± 0.02	$101.6 \pm 0.1^*$	100.7 ± 0.1
BD +404124	B2	$1.22 \pm 0.01^*$	1.37 ± 0.01	$8.7 \pm 0.2^*$	17.4 ± 0.2
ω Ori	B3 III–IV	$0.27 \pm 0.01^\bullet$	0.77 ± 0.01	$55.7 \pm 0.6^\bullet$	43.9 ± 0.1
MWC 147	B6 V	$1.05 \pm 0.01^*$	0.85 ± 0.01	$100.0 \pm 0.1^*$	102.4 ± 0.1
AB Aur	A0 V	$0.11 \pm 0.01^*$	0.24 ± 0.01	$53.3 \pm 0.9^*$	54.5 ± 0.6
MWC 120	A0	0.41 ± 0.01	0.40 ± 0.01	115.4 ± 0.2	117.0 ± 0.1
MWC 480 1	A2	0.20 ± 0.01	0.33 ± 0.01	64.9 ± 1.3	64.3 ± 0.6
XY Per	A2 II	$1.60 \pm 0.01^*$	1.60 ± 0.01	$131.6 \pm 0.1^*$	125.5 ± 0.1

* Data from Vink et al. (2002), \bullet data from Oudmaijer & Drew (1999)

calibration was performed using several calibration spectra (obtained by observing a Copper-Argon-Neon lamp) taken throughout the observing runs. The images were then imported into the Starlink program CCD2POL, which is part of the Time-Series/Polarimetry (TSP) package, in order to obtain the Stokes parameters for each polarisation set. The resultant data was then fed into the POLMAP package also maintained by Starlink, in order to measure the polarisation and polarisation angle, and to produce plots of the data.

The objects observed included several polarisation and zero-polarisation standards. These were observed so that the instrumental polarisation and instrumental polarisation angle could be measured by comparing the initial results for these objects with the literature. From these data, we found that the polarisation P has a systematic error of $\simeq 0.1\%$ and the polarisation angle θ has a systematic error of $\leq 1^\circ$. While in principle the achieved accuracy is governed by photon statistics alone as \sqrt{N} (typically 0.01%), it can be seen that these calibration and telescope-induced errors are the main limiting factor.

We do not correct for instrumental or interstellar polarisation because these only add a wavelength-independent constant to the Stokes Q and U parameters. Due to this wavelength independence, we concentrate on the (Q, U) representation of the hydrogen emission line polarisation signatures when classifying the observed behaviour. Furthermore, it is often not possible to distinguish the effects of the interstellar medium from that of the material immediately surrounding the target object such as dust.

3 RESULTS

We have listed the observational properties for both the R and B band observations for all Herbig Ae and Be stars in Table 1. For 9 of the 12 objects, additional R band data from Vink et al. (2002) and Oudmaijer & Drew (1999) have been listed. For 3 objects, H α data were taken in 2004.

The continuum polarisation was measured for all targets in both B and R , and is listed in Table 2. This acts as a reasonable indicator of variability, although some intrinsic difference is expected between the two bands. In some cases, the data from different epochs show little variation and a direct comparison is possible. For those cases in which time-variability might be an issue, we will discuss the possible implications. Line characteristics, polarisation effect properties and the measured intrinsic polarisation, where possible, are summarised for all objects in Table 3.

In the following section, we first provide a brief discussion regarding the definition of observed line effects (§ 3.1), before we present the polarisation data of our Herbig Ae/Be objects, highlighting representative data for some individual objects in § 3.2 and § 3.3, while we present the remaining data with accompanying notes in the Appendix. We finish the section with a global comparison between Herbig Ae and Herbig Be stars (§ 3.4).

3.1 Line Effect Characterisation

In order to characterise the observed line effects in terms of “depolarisation” or “ QU loop”, we briefly discuss the definitions, following the method first used in Vink et al. (2002). For depolarisation, the line effect needs to be broad compared to the emission line. If a PA ‘flip’ occurs, i.e. a sharp change in the profile from above to below continuum levels, or vice versa, then this cannot be caused by depolarisation, but the line itself must be intrinsically polarised.

In QU space, the following classification can be followed: where no change in polarisation or PA is observed, the QU loci appear as a ‘spot’. In the case of a depolarisation, a linear excursion from, and returning to, the central spot is observed (e.g. see the top three panels in Fig. 3), whilst in the case of a PA ‘flip’, a loop is observed in QU space (e.g. see the bottom three panels of Fig. 3).

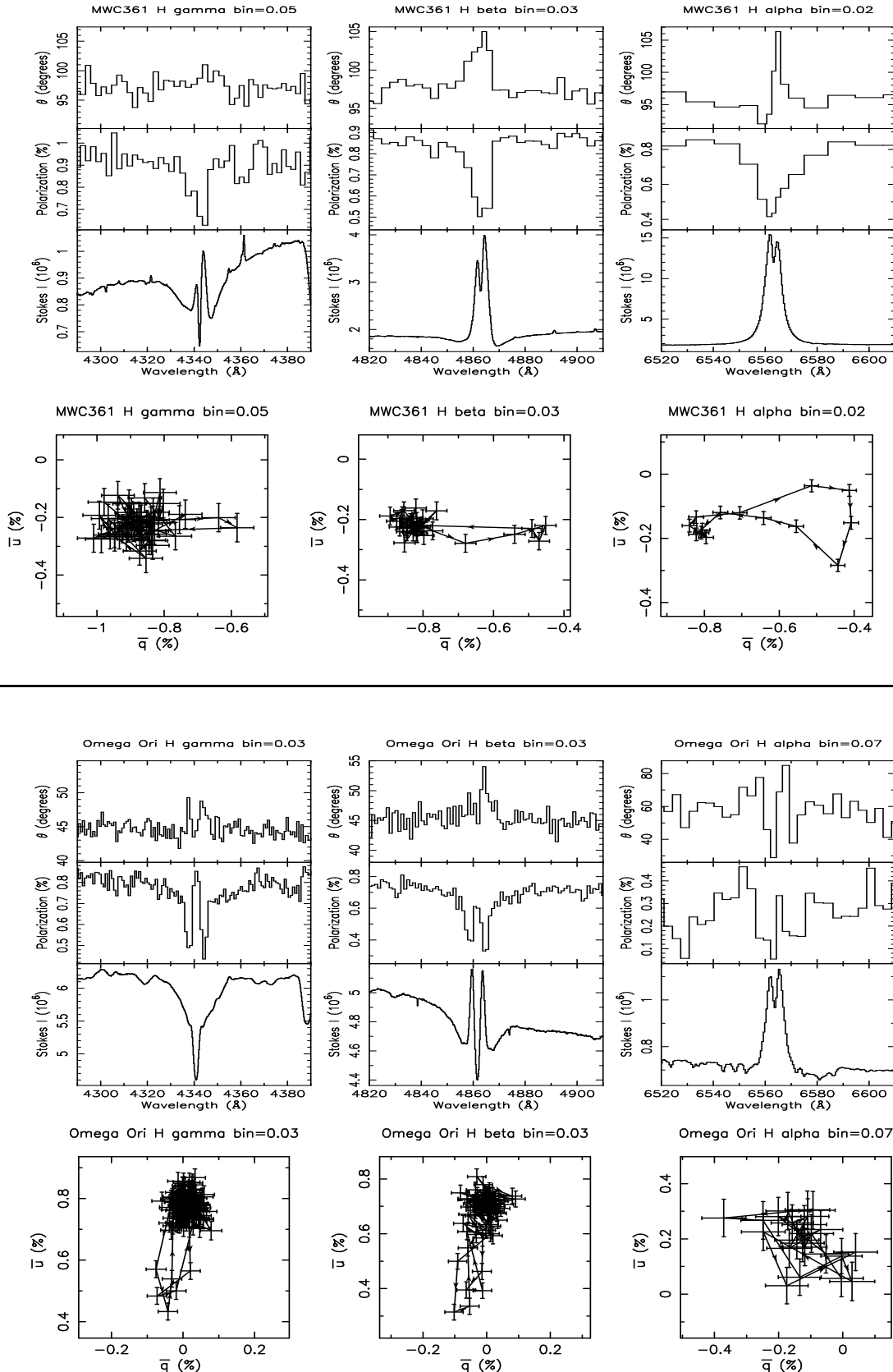


Figure 1. The polarisation data of two Herbig Be stars. The H α data for MWC 361 is from 1999 and of ω Ori is from 1995. The H β and H γ data of both objects were taken in 2004. Top figures: the data are visualised using “triplots” (top) and (Q, U) diagrams (bottom) of MWC 361 around H γ , H β and H α . In the polarisation spectra, the bottom panel shows the Stokes intensity as a function of wavelength, while the middle panel shows the percentage polarisation and the upper plot the polarisation angle, also as function of wavelength. Bottom figures: as above, but now for ω Ori. The difference between the B and R band continuum data (see table 2) suggests that the emission from the object is variable (see text). Note that the H γ emission is hardly visible, but still yields a polarisation signature

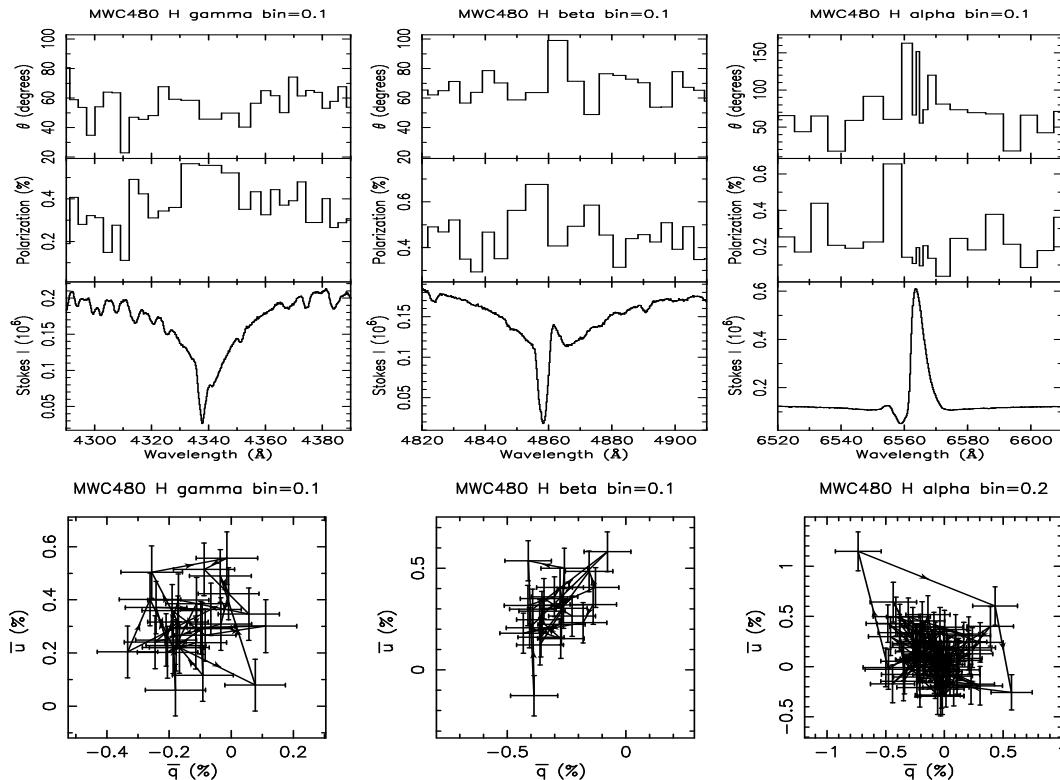


Figure 2. As in Fig. 1 but for the Herbig Ae star MWC 480. The binning error for the (Q, U) plot for $H\alpha$ is twice that of the triplot in order to provide a well-defined continuum. All data is from 2004.

3.2 Herbig Be polarimetry at $H\gamma$, $H\beta$ and $H\alpha$

Figure 1 shows first the polarisation data for MWC 361 in the top panels. This object has the clearest depolarisation line effects in the sample and is therefore an excellent example to start the description.

The top half of the figure shows, from left to right, the data on $H\gamma$, $H\beta$ and $H\alpha$ respectively. The triplots show from bottom to top the intensity spectrum, the polarisation percentage and polarisation angle rebinned to a constant accuracy per pixel, which is shown to the top right of each plot. Below the triplots, the QU graphs are shown.

As expected, the line emission is stronger when going to lower order recombination lines. Indeed, $H\gamma$ emission is obviously present, but barely exceeds the continuum, as it fills in the underlying photospheric absorption line. Nevertheless, even the $H\gamma$ line shows a depolarisation similar to $H\alpha$, despite its much smaller transition probability. The intrinsic polarisation measured from the line excursions is -3° and 3° (with errors of order 3°) respectively for the B and R band data. In all bands, the line-effect is best described as depolarisation, although there is a somewhat more complex structure in $H\alpha$ (see Vink et al. 2002).

The continuum polarisation and PA across the R and B bands are quite similar, with the difference being mainly due to the slight difference in intrinsic PA between the epochs of observation. The behaviour in QU space is also very similar across all three lines, although the blue-to-red line ratio has changed between the two observations. Based on the similar depolarisations in the polarisation spectra as well as the similar excursion in QU space, we conclude that the (de-) polarisation mechanism responsible for the appearance at $H\alpha$

is also acting at $H\beta$ and $H\gamma$. Therefore, a small-scale electron scattering disc, seen close to edge-on, is the most plausible explanation for the phenomena observed in MWC 361.

Let us now move to the data for ω Ori, which are plotted in the lower panels of Fig. 1. This object shows depolarisation in our data at both $H\beta$ and $H\gamma$, but it does not show any appreciable effect in the R band data of Oudmaijer & Drew (1999) taken nine years earlier. However, Poeckert & Marlborough (1975) do observe a polarisation change at $H\alpha$ and closer examination of the QU plots shows that the end of the excursions at both $H\beta$ and $H\gamma$ lie near the continuum cluster for $H\alpha$ of Oudmaijer & Drew (1999). This corroborates their suggestion that the decreased emission level at $H\alpha$ at the time of observation resulted in a marked drop in the percentage of linearly polarised scattered starlight from the star.

Also noteworthy is the fact that we see a line effect at $H\gamma$ in the first place, although the line is in absorption. For an ordinary main-sequence star of the same spectral type as ω Ori, $H\beta$ and $H\gamma$ are in absorption. The line effect across $H\beta$ appears to coincide only with the emission peaks, and not with the absorption at line centre. There is some weak emission at $H\gamma$ as well - there is just not enough to fill in the absorption. Never before has such a weak emission line been observed to have a polarisation effect. This indicates that, as long as the data is of a high enough quality, only moderate amounts of emission are needed to cause a detectable line effect.

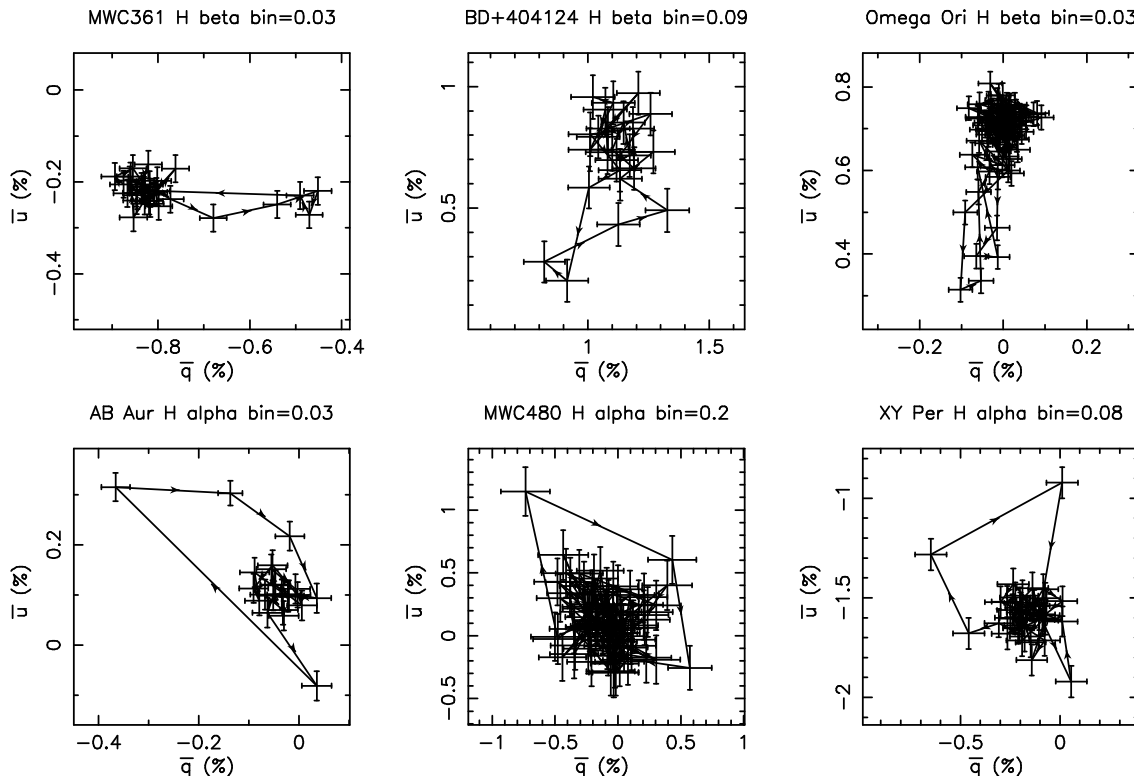


Figure 3. QU data for the three Herbig Be stars with the strongest line effect in $H\beta$ (top) and a representative sample of $H\alpha$ data of Herbig Ae stars. The Herbig Be stars show linear excursions, while the Herbig Ae stars display loops.

3.3 Herbig Ae stars at $H\gamma$, $H\beta$ and $H\alpha$

We obtained data in both the B and R band during the same run of the Herbig Ae star MWC 480, and these are shown in Fig. 2. MWC 480 shows no line effects in the B band, but a strong line effect at $H\alpha$ is present. Contrary to the objects discussed above, the appearance in QU space is that of a loop. There is evidence of emission at both $H\beta$ and $H\gamma$, and as we showed in the previous subsection, if there would have been a line effect, our fairly high signal-to-noise data might have revealed it. In the case of the Herbig Be stars, the polarisation is due to electron scattering in a disc, which does not result in a loop in the QU diagram. The non-detection in these lines, while we do find an intrinsic line effect at $H\alpha$ data taken nearly simultaneously is a further indication that the polarisation mechanism in Herbig Ae stars may be different from that in the earlier objects.

3.4 Brief overview of results

For five out of the eight Herbig Be stars that have been observed at $H\beta$, we observe depolarisations. A comparison with existing $H\alpha$ data shows that the intrinsic polarisation angle is similar at both $H\alpha$ and $H\beta$. In one case, no line-effect was detected previously at $H\alpha$, but there does seem to be one at shorter wavelengths now. This is most likely due to the intrinsic variability of the hydrogen recombination emission. The detection statistic, that more than half, but not all, of the objects are found to show a line effect is consistent with previous studies such as Vink et al. (2002);

Oudmaijer & Drew (1999) and Poekert & Marlborough (1975).

Only one of the Herbig Ae type stars displays a line effect at $H\beta$ (MWC 120, with a spectral type of A0, the earliest Herbig Ae star). All four objects show polarisation effects at $H\alpha$ in the form of a QU loop.

4 DISCUSSION

4.1 General Trends

As has been shown by Vink et al. (2002), and additional data of Vink et al. (2005a), the vast majority of Herbig Ae stars (10 out of 13) that display a line-effect at $H\alpha$ show a loop in the QU diagram. Our new data on Herbig Ae stars indicate that the $H\alpha$ signatures are again of the loop variety, but we note that in the present data the line-effect for MWC 120 is not as clear as when it showed a loop in the older data of Vink et al. (2002). On the other hand, the overwhelming majority of Herbig Be objects (five out of seven) show depolarisations at $H\alpha$. The only Herbig Be star that shows a loop (HD 58647 in Vink et al. 2002) has a late-B spectral type (B9). The $H\alpha$ line of Herbig Be stars is very strong, with the line-to-continuum contrasts of these objects generally exceeding 10 (see Vink et al. 2002), whereas the $H\alpha$ line in the Herbig Ae stars is not so strong, with typical line-to-continuum contrasts in the range 3-4.

For the Herbig Be stars, our main finding is that for all cases where a line effect was found, the Herbig Be stars show the *same* type of line effect at $H\beta$ and $H\gamma$ as was found earlier at $H\alpha$. MWC 147 with a spectral type of B6 may be

Table 3. H line results. Columns 2-4 contain the equivalent widths, (with errors below 5 per cent). Columns 5-7 indicate whether a line effect is observed, and columns 8-11 give the shape of the corresponding loci in QU space for a given emission line (defined in Vink et al. 2002). Columns 12 & 13 give the intrinsic polarisation angle, calculated by measuring Q and U for the continuum and emission line for excursion line effect, using $\theta(^{\circ}) = \frac{1}{2} \arctan \left(\frac{\Delta U}{\Delta Q} \right)$.

Object Name	EW(Å)			Line effect?			QU behaviour			$\Theta_{intr}(^{\circ})$	
	H α	H β	H γ	H α	H β	H γ	H α	H β	H γ	R	B
MWC 166	-14	2.9	3.5	Y	N	N	Exc	-	-	136 ± 4	-
MWC 1080 ¹	-	-14	-1.1	-	Y	Y	-	Smear	Smear	-	$158 \pm 14^*$
MWC 1080 ²	-100	-15	-1.4	Y	Y	Y	Smear	Smear	Smear	165 ± 4	$164 \pm 12^*$
GU CMa	-14	3.8	4.8	N	N	N	-	-	-	-	-
MWC 361	-65	-2.5	3.2	Y	Y	Y	Exc	Exc	Exc	3 ± 2	$177 \pm 4^*$
II Cep	-21	3.4	4.5	N	N	N	-	-	-	-	-
BD +404124	-120	-10	-0.60	Y	Y	N	Exc	Exc	-	36 ± 3	37 ± 6
ω Ori	-2.9	1.1	2.6	N	Y	Y	-	Exc	Exc	-	$36 \pm 2^*$
MWC 147	-65	-2.3	2.4	Y	Y	N	Exc/Loop?	Exc	-	168 ± 4	21 ± 13
AB Aur	-32	15	16	Y	N	N	Loop	-	-	-	-
MWC 120	-20	7.6	9.5	Y	Y	Y	Loop	Loop	Loop	-	-
MWC 480	-11	16	16	Y	N	N	Loop	-	-	-	-
XY Per	1.9	16	13	Y	N	N	Loop	-	-	-	-

¹ 28/09/2004, ² 29/09/2004, * average over H β and H γ

an exception; the results are inconclusive. An illustration of the differences between Herbig Be and Ae stars is provided in Fig. 3. Here we compare the H β line in Herbig Be stars, and the H α line in Herbig Ae stars, as these lines are rather comparable in strength, yet we find a marked difference in the character of their line effects. This suggests that transition probability and optical depth do not appear to affect the type of line effect observed, and the H α feature alone should be sufficient to decide between intrinsic line polarisation (present in the Herbig Ae/T Tauri stars) and depolarisation (seen in the Herbig Be stars).

These line polarisation effects may then be used as a tool to determine whether the underlying accretion process is likely to be magnetospheric, or more characteristic of disc accretion, as motivated in the following. We attribute the QU loops of the Herbig Ae/T Tauri stars to magnetospheric accretion for a number of reasons. First of all, the line is only then expected to be intrinsically polarised if the photons originate *interior* to the scatterers. i.e. a compact source of line photons should be available. Secondly, the QU loops indicate that the scatterers are situated in a rotating geometry, most likely the accretion disc surrounding the central star, but this is not all: Vink et al. (2005b) recently showed that a disc that reaches the star at its equator would show *double* PA flips rather than *single* ones. This indicates that the line polarimetry behaviour observed in the Herbig Ae/T Tauri stars is only expected when the accretion disc has an inner hole. Even more so, Vink et al. (2005a) constrained the sizes of these inner holes and found these to be compatible with magnetospheric radii.

The depolarisation data seen in the Herbig Be stars hint at an altogether different circumstellar geometry. First of all, the compact source of line photons is missing, whilst secondly, the continuum polarisation suggests the occurrence of electron scattering within a few stellar radii. All in all, the depolarisation data seen in the early Herbig Be stars are consistent with the presence of a disc, and so suggest for-

mation by disc accretion. Observations in the spectral range of B4-B9 could help us understand what could cause this possible shift from magnetospheric accretion in Herbig Ae stars to disc accretion in early Herbig Be stars.

4.2 Comparison with other diagnostics

We presented spectropolarimetric data on eight Herbig Be stars at H α , H β and H γ , and we found five cases where the behaviour could be described as “depolarisation”. Two Herbig Be stars show no polarisation line effects, and only one transitional object (at spectral type B6) may show hints of a (Q, U) loop. Furthermore, the observed line effects are consistent across all three observed hydrogen lines, indicating that optical depth is not a major factor in the observed linear polarimetry across emission lines in Herbig stars. This leads us to conclude that it is most likely that a different accretion mechanism is operating in Herbig Be stars than in Herbig Ae stars.

The fact that the role of magnetic fields may be diminishing when going to earlier spectral types could, at first sight, be considered at odds with the fact that up to 30 - 50% of Herbig stars were found to be significant emitters of X-rays (Damiani et al. 1994; Zinnecker & Preibisch 1994), some of which have very early B-types. However, the higher spatial resolution of current X-ray satellites, in particular CHANDRA, can be utilised to investigate whether the X-ray photons are intrinsic to the Herbig star, or whether they are originating from a low-mass companion (see e.g. Stelzer et al. 2006). In a recent infrared (IR) coronagraphic imaging and CHANDRA study of the extremely early Herbig Be star MWC 297, Vink et al. (2005c) and Damiani et al. (2006) have argued that the X-rays likely originate from a low-mass companion. Interestingly, an increase in the number of low-mass companions (“clustering”) with stellar mass and spectral type amongst Herbig stars was found by Testi et al. (1998), which Vink et al. (2005c) considered as

yielding a higher chance for misidentification of X-rays towards earlier type Herbig stars. Therefore, the current status on the origin of X-rays of Herbig Ae/Be stars suggests that T Tauri and some Herbig Ae stars may be intrinsic X-ray emitters (e.g. Swartz et al. 2005), while early Herbig Be stars are likely not.

This picture on the X-rays from Herbig stars as a function of spectral type can be reconciled with the linear spectropolarimetry results presented in this paper if there is a “fading” of the importance of magnetic fields at spectral types earlier than B4-B9. It is interesting, however, that Wade et al. (2006) recently reported the detection of a significant magnetic field in the Herbig Be star MWC 361, as this is also the object for which Vink et al. (2002) found a narrow PA rotation in the red wing of $H\alpha$, on top of an otherwise well-defined depolarisation.

We finally mention that infrared interferometry observations by Monnier et al. (2005) suggest that the early Herbig Be stars (B0-B3) are discrepant in terms of the “disc size - source luminosity relationship” that works so well for Herbig Ae and late Herbig Be systems. This discrepancy could possibly be caused by the fact that different accretion scenarios are operating in the early Herbig Be stars and the Herbig Ae stars.

This appears to be in line with the line polarimetry data of Herbig Ae/Be stars currently available: the Herbig Ae stars show intrinsic line polarisation, similar to T Tauri stars, and consistent with magnetospheric accretion, while the majority of Herbig Be stars show depolarisation, consistent with disc accretion.

ACKNOWLEDGEMENTS

We thank the referee for comments that improved the clarity and contents of this paper and Prof. Janet Drew for many fruitful discussions. JCM would like to thank Ben Davies for help with POLMAP. The William Herschel Telescope is operated on the island of La Palma by the Isaac Newton Group in the Spanish Observatorio del Roque de los Muchachos of the Instituto de Astrofísica de Canarias. The allocation of time on the WHT was awarded by PATT, the United Kingdom allocation panel. Data analysis facilities were provided by the Starlink Project, which is run by CCLRC on behalf of PPARC. JCM is funded by the Particle Physics and Astronomy Research Council of the United Kingdom. JSV acknowledges RCUK for an Academic fellowship.

REFERENCES

- Baines D., Oudmaijer R.D., Porter J.M., Pozzo M., 2006, *MNRAS*, 367, 737
- Damiani F., Micela G., Sciortino S., Harnden F.R., 1994, *ApJ*, 436, 807
- Damiani F., Micela G., Sciortino S., 2006, *A&A*, 447, 1041
- Hubrig S., Yudin R.V., Schöller M., Pogodin M.A., 2006, *A&A*, 446, 1089
- Johns-Krull C.M., Valenti J.A., Hatzes A.P., Kanaan A., 1999, *ApJ*, 510, L41
- Monnier J.D., Millan-Gabet R., Billmeier R. et al., 2005, *ApJ*, 624, 832
- Monet D.G., Levine S.E., Canzian B. et al., 2003, *AJ*, 125, 984
- Natta A., Prusti T., Neri R., Wooden D., Grinin V.P., Mannings V., 2001, *A&A*, 371, 186
- Oudmaijer R.D., Drew J.E., 1999, *MNRAS*, 305, 166
- Poeckert R., Marlborough J.M., 1976, *ApJ*, 206, 182
- Stelzer B., Micela G., Hamaguchi K., Schmitt J.H.M.M., 2006, *A&A*, 457, 223
- Swartz D.A., Drake J.J., Elsner R.F. et al., 2005, *ApJ*, 628, 811
- Symington N.H., Harries T.J., Kurosawa, R., Naylor T., 2005, *MNRAS*, 358, 977
- Testi L., Palla F., Natta A., 1998, *A&AS*, 133, 81
- Thé P.S., de Winter D., Perez M.R., 1994, *A&AS*, 104, 315
- Vink J.S., Drew J.E., Harries T.J., Oudmaijer R.D., 2002, *MNRAS*, 337, 356
- Vink J.S., Drew J.E., Harries T.J., Oudmaijer R.D., Unruh Y., 2005a, *MNRAS*, 359, 1049
- Vink J.S., Harries T.J., Drew J.E., 2005b, *A&A*, 430, 213
- Vink, J.S., O’Neill P.M., Els S.G., Drew J.E., 2005c, *A&A*, 438, L21
- Wade G.A., Drouin D., Bagnulo S. et al., 2005, *A&A*, 442L, 31
- Wade G.A., Drouin D., Bagnulo S., et al., 2006, *astro-ph/0601624*
- Zinnecker H., Preibisch Th., 1994, *A&A*, 292, 152

APPENDIX A: NOTES ON INDIVIDUAL OBJECTS

A1 Herbig Be Stars

MWC 361 & MWC 1080

These objects show line effects at all observed lines. For MWC 1080 (Fig. A1) though these are shallow and quite broad, except in the case of $H\gamma$ on 29/04/2004. There is an increase in B band continuum polarisation between the two nights of observation, but despite the large difference in continuum polarisation between B and R , the intrinsic PA agrees with the data taken on the 29th. The shape of the depolarisation effect and (Q,U) smear are similar to those observed by Vink et al. (2002), although the R band continuum polarisation they record is noticeably higher. They attribute the smear in the (Q,U) diagram to changing continuum polarisation, which is notable between R and B in our observations and, to a lesser extent, across the bands themselves. MWC 1080 would seem to be quite variable on short timescales, and is a known binary system (Baines et al. 2006, and references therein) so will probably exhibit long term variations as well.

MWC361 was discussed previously in section 3.2.

BD +404124, MWC 147, MWC 166 & ω Ori

These objects show line effects at only some of the observed lines. BD +404124 shows (Fig. A1) depolarisation at $H\alpha$ and $H\beta$, with corresponding excursions in the (Q,U) plots, but there are no more than vague suggestions of a line effect at $H\gamma$. Both the continuum polarisation and PA increase slightly in the B band from the R band observations, possibly causing the slight change in shape of the line effect between $H\alpha$ and $H\beta$. There is, however, clear and quite

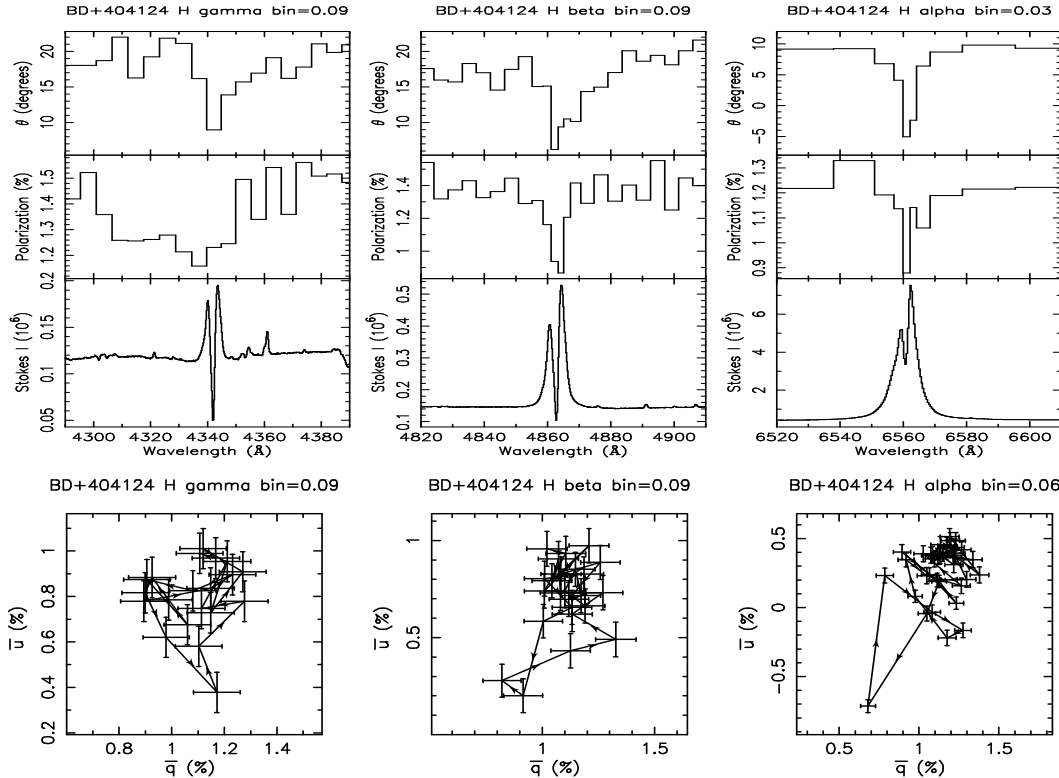
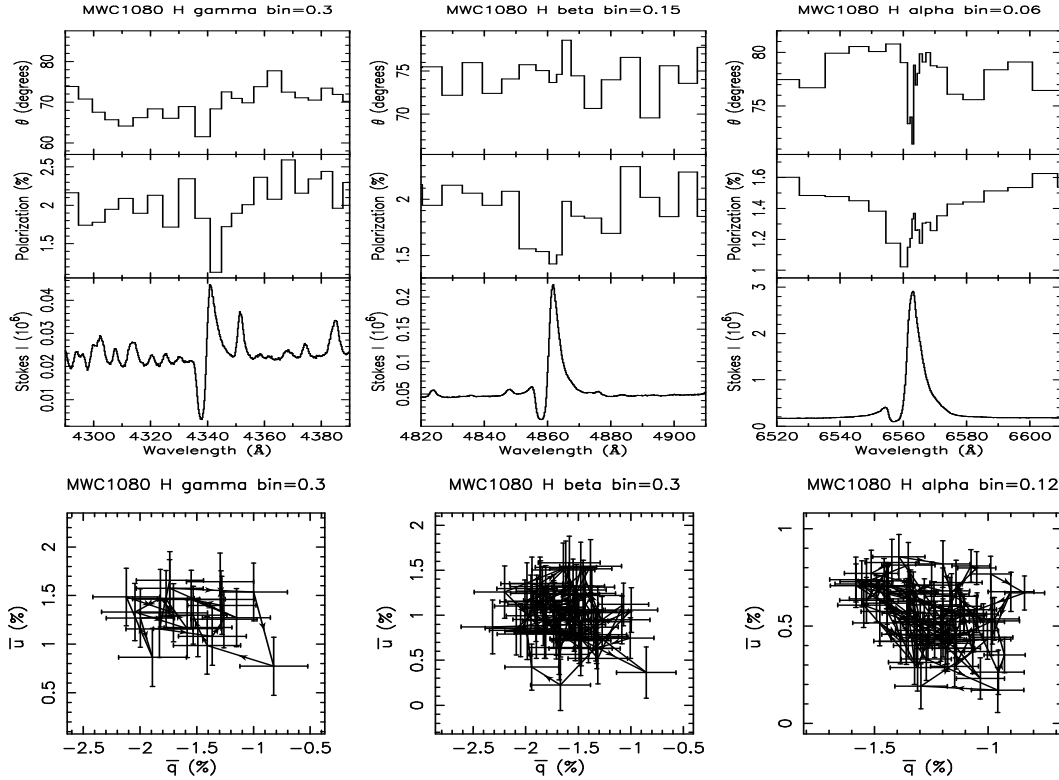


Figure A1. Herbig Be Stars. Top figures: as in Fig. 1 but for MWC 1080 around $H\gamma$, $H\beta$ and $H\alpha$ on 29/09/2004. The binning errors for the (Q,U) plot for $H\alpha$ and $H\beta$ are twice that of the triplet in order to provide a well-defined continuum. This data is consistent with that taken on 28/09/2004. Bottom Figures: as above but for BD +404124 around $H\gamma$, $H\beta$ and $H\alpha$. The binning error for the (Q,U) plot for $H\alpha$ is twice that of the triplet in order to provide a well-defined continuum. The $H\alpha$ data is from 1999 while the $H\beta$ and $H\gamma$ data is from 2004.

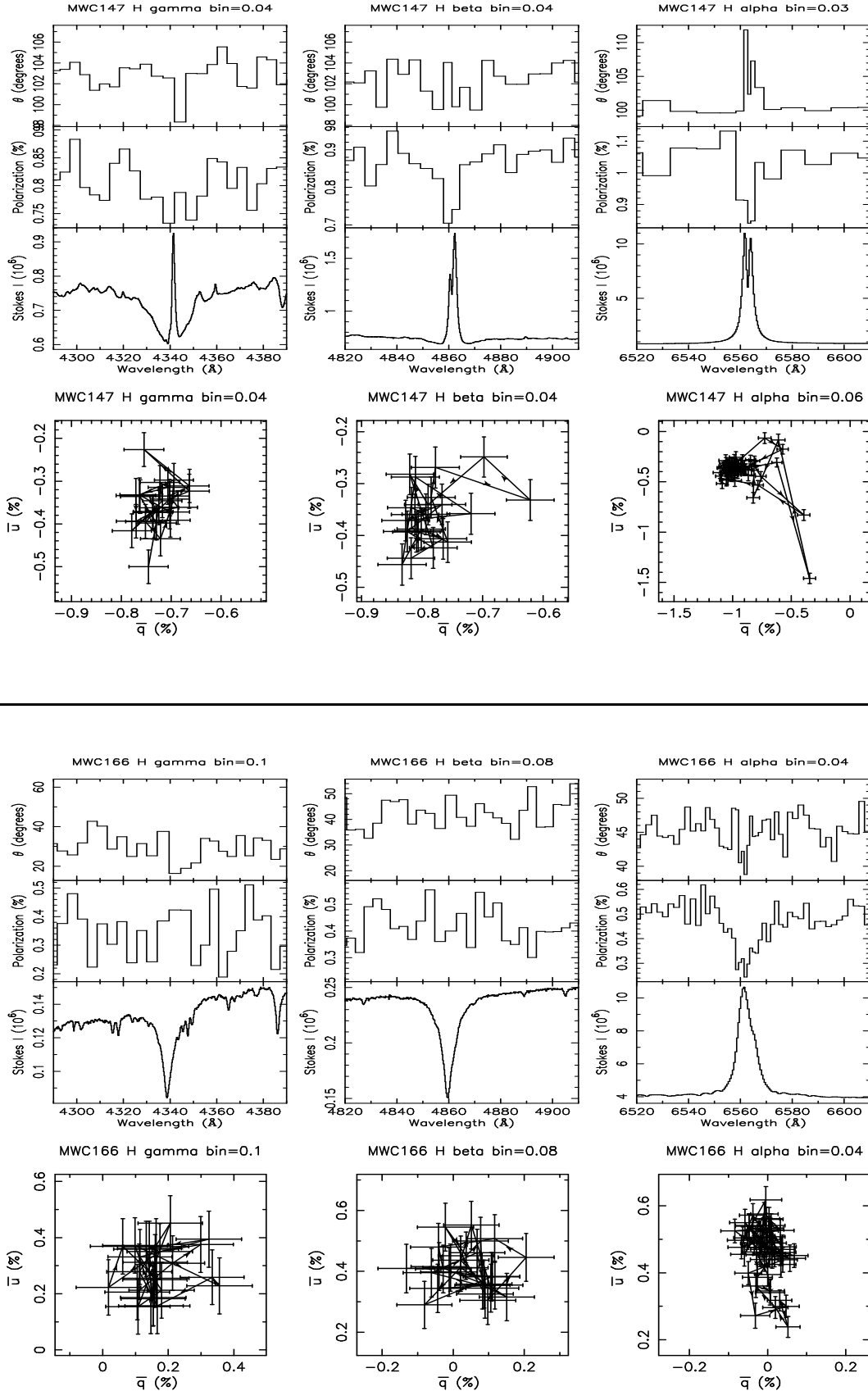


Figure A1. Cont. Herbig Be Stars. Top figures: as in Fig. 1 but for MWC 147 around H γ , H β and H α . The binning error for the (Q,U) plot for H α is twice that of the triplot in order to provide a well-defined continuum. The H α data is from 1999 while the H β and H γ data is from 2004. Bottom Figures: as above but for MWC 166 around H γ , H β and H α . The H α data is from 1996/7 while the H β and H γ data is from 2004.

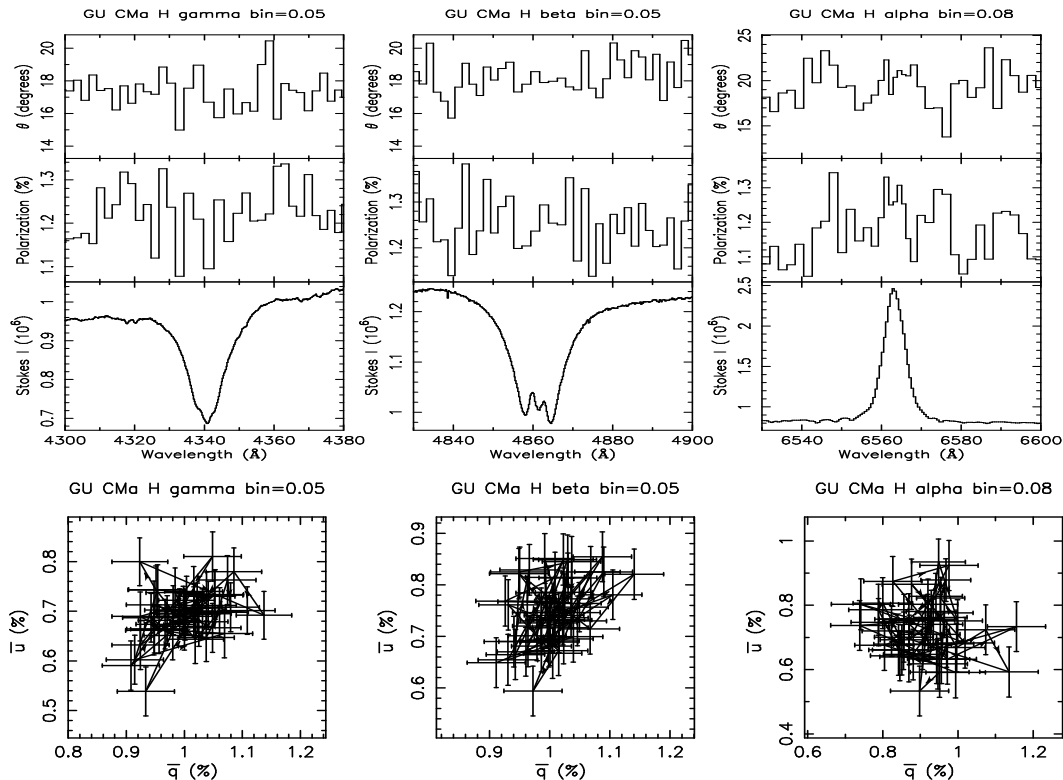


Figure A2. Herbig Ae Stars. As in Fig. 1 but for GU CMa around $H\gamma$, $H\beta$ and $H\alpha$. The $H\alpha$ data is from 1995 while the $H\beta$ and $H\gamma$ data is from 2004.

strong emission at all three lines, so the lack of a clear effect at $H\gamma$ is most likely due to the faintness of BD +404124 and may become apparent with longer exposure observations.

The first point of interest for MWC 147 is the fact that the emission lines have different shapes in the R and B bands (Fig. A1). $H\alpha$ (observed 18/12/1999) is double peaked with a V/R peak ratio > 1 , i.e. $V > R$, while $H\beta$ (observed 28/09/2004) is double peaked with $V < R$. $H\gamma$ appears single peaked, with the emission slightly displaced to the R side of the absorption feature. This difference between $H\alpha$ and $H\beta$ is probably due to time variability. There are definitely line effects at $H\alpha$ and $H\beta$, with little sign of effects at $H\gamma$, but it is unclear if the effects are depolarisation effects, or QU loops. This makes it difficult to say if MWC 147 is more likely accreting via magnetospheric accretion or via disc accretion.

For MWC 166, a depolarisation is observed at $H\alpha$ while no line effects are observed in the B band (Fig. A1). The continuum polarisation in the B band is lower than at R , to the point where the continuum polarisation in B is near the bottom of the depolarisation at $H\alpha$. In addition, there are only slight indications of emission at $H\beta$ or $H\gamma$. Overall, it is to be expected that we do not see line effects for MWC 166 in B , with the differences possibly caused by variations in the object between the two observations.

ω Ori was discussed previously in section 3.2.

GU CMa & Il Cep

Neither GU CMa (Fig. A2), nor Il Cep (Fig. A2) show any sign of line effects in either the B or R band. Although the R band data was taken at a different epoch to the

B band data, the continuum polarisation percentage and PA agree, which suggests little change in the circumstellar medium around the object between these observations. The high level of continuum polarisation of the objects, $\sim 1.2\%$ for GU CMa and $\sim 4.2\%$ for Il Cep, and the high quality of the data means that it is unlikely that these objects exhibit undetected line effects, and their electron scattering discs are expected to be relatively pole-on.

A2 Herbig Ae Stars

AB Aur, MWC 120, MWC 480 & XY Per

These objects have line effects at only some of the observed lines. AB Aur shows clear line effects in the $H\alpha$ data of Vink et al. (2002) but we observe no line effects in our B band data (Fig. A2). The continuum polarisation has increased considerably, although Vink et al. (2005a) see line effects at $H\alpha$ in Dec 2003 with a level of continuum polarisation in R similar to ours. Therefore, while the polarisation level around AB Aur has increased, it should not have prevented detection of the line effect. There are signs of emission in the $H\beta$ and $H\gamma$ profiles, but it is possible that it is simply not high enough for an A type star, which tend to have broader and deeper absorption lines and lower continuum emission at these wavelengths than B type stars.

MWC 120 shows the suggestion of a line effect at $H\gamma$ and clear line effects at the other two observed lines (Fig. A2). The V/R ratio appears to be similar in both $H\beta$ and $H\alpha$, and there are signs of some emission at $H\gamma$. The data is of quite a high signal-to-noise, so longer exposure may not improve the definition of the possible effect at $H\gamma$.

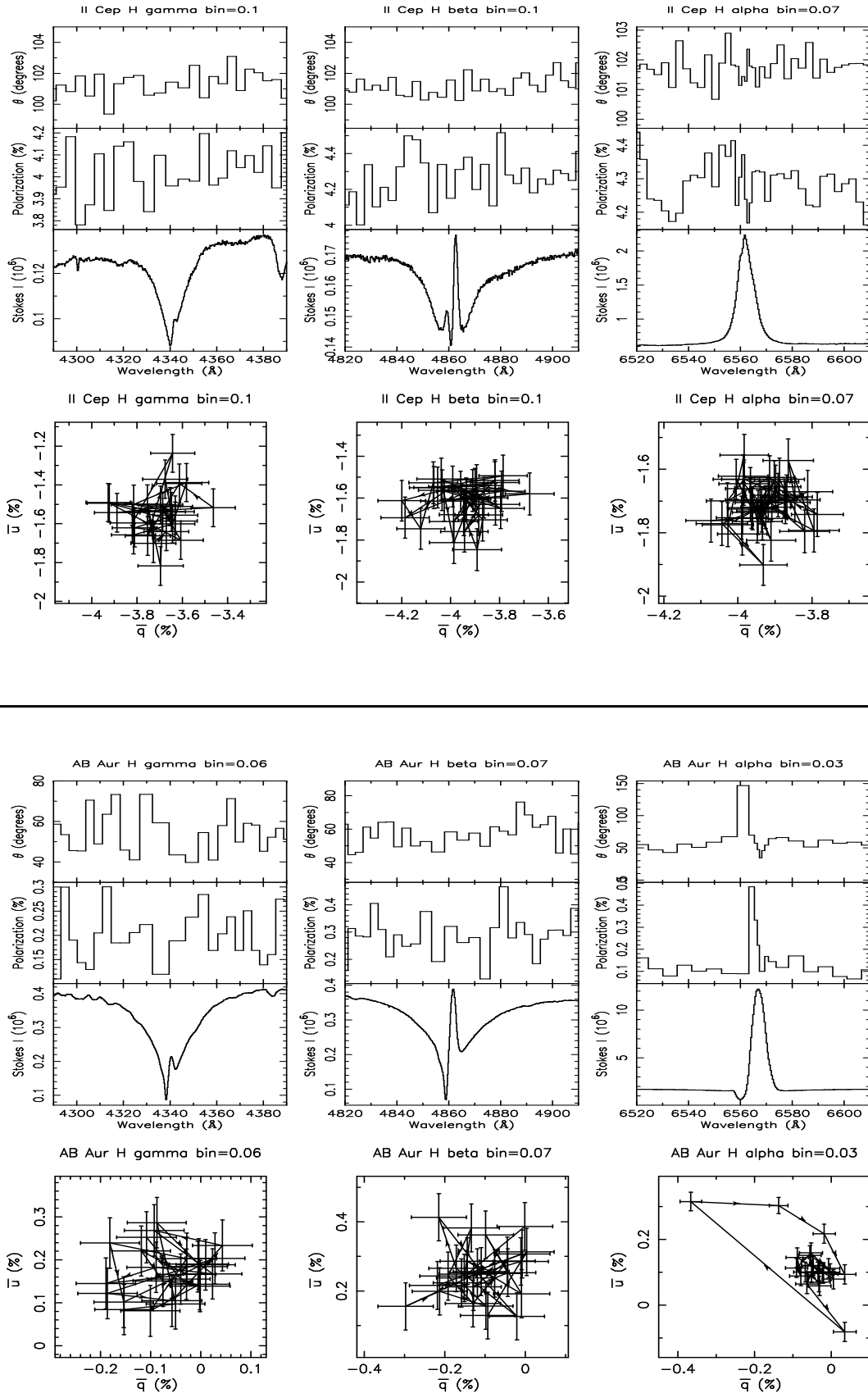


Figure A2. Cont. Herbig Ae Stars. Top figures: as in Fig. 1 but for II Cep around H γ , H β and H α . The H α data is from 1999 while the H β and H γ data is from 2004. Bottom figures: as above but for AB Aur around H γ , H β and H α . The H α data is from 1999 while the H β and H γ data is from 2004.

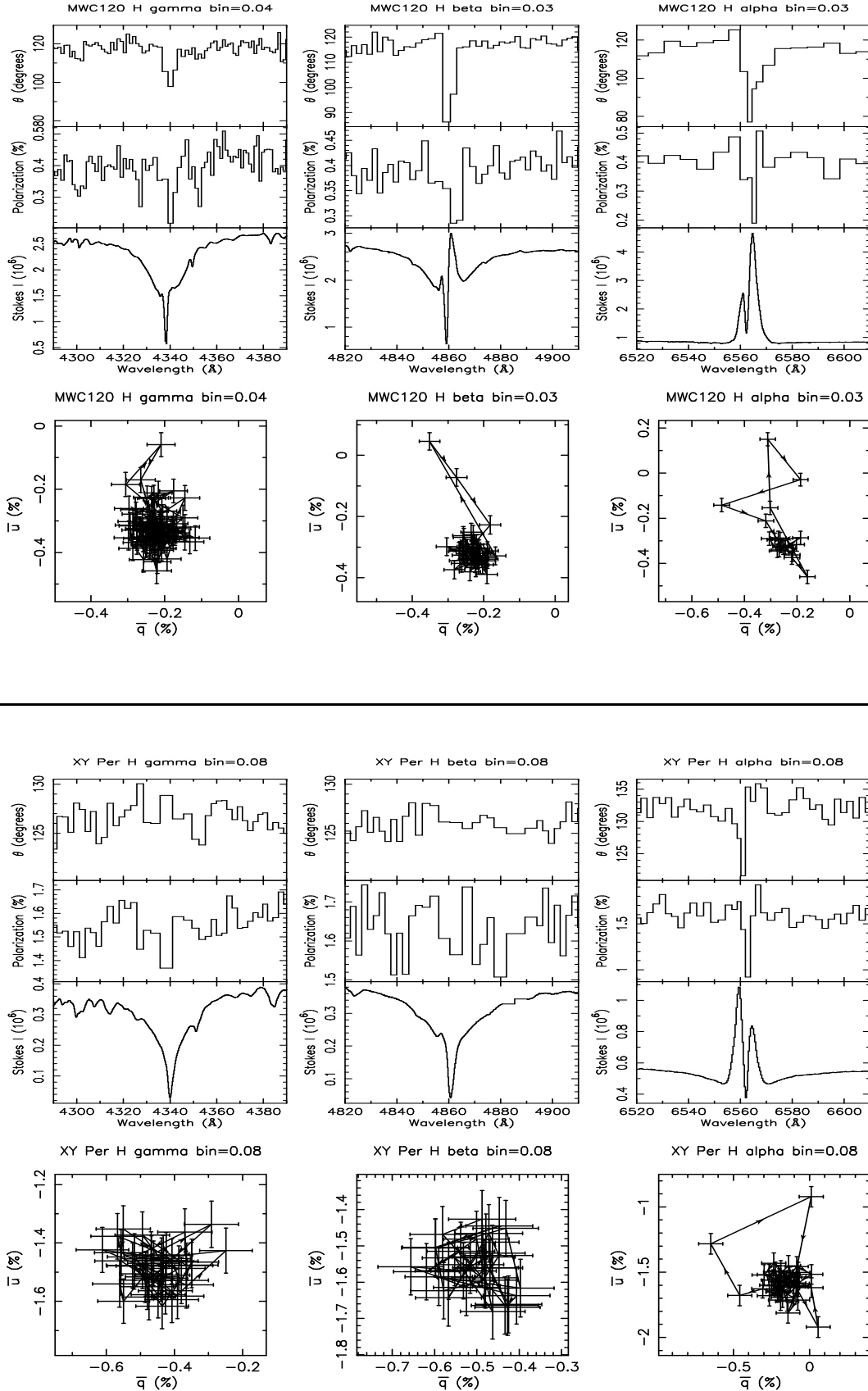


Figure A2. Cont. Herbig Ae Stars. Top figures: as in Fig. 1 but for MWC 120 around H γ , H β and H α . All data is from 2004. Bottom figures: as above but for XY Per around H γ , H β and H α . The H α data is from 1999 while the H β and H γ data

XY Per shows no sign of line effects in B but does show line effects at $H\alpha$ (Fig. A2). The continuum polarisation is consistent between the two observed bands, and there are few signs of emission in the B band line profiles, suggesting that there are too few photons for a signature to be observed.

MWC 480 was discussed previously in section 3.3